Developmental Biology 339 (2010) 89–100

Contents lists available at ScienceDirect

Developmental Biology

journal homepage: www.elsevier.com/developmentalbiology

Deficiency of *smarcal1* causes cell cycle arrest and developmental abnormalities in zebrafish

Cheng Huang [a,d,*], Shanye Gu [b], Pengchun Yu [b], Fudong Yu [c], Chun Feng [a], Ning Gao [e], Jiulin Du [b,*]

[a] Institute for Nutritional Sciences and Key Laboratory of Nutrition and Metabolism, Shanghai Institutes for Biological Sciences, Chinese Academy of Sciences, Shanghai 200031, China
[b] Institute of Neuroscience and State Key Laboratory of Neuroscience, Shanghai Institutes for Biological Sciences, Chinese Academy of Sciences, Shanghai 200031, China
[c] Bioinformatics Center and Key Laboratory of Systems Biology, Shanghai Institutes for Biological Sciences, Chinese Academy of Sciences, Shanghai 200031, China
[d] School of Pharmacy, Shanghai University of Traditional Chinese Medicine, 1200 Cailun Road, Shanghai 201203, China
[e] Department of Pharmacognosy, School of Pharmacy, Third Military Medical University, 30 Gaotanyan Street, Chongqing 400038, China

ARTICLE INFO

Article history:
Received for publication 24 March 2009
Revised 14 December 2009
Accepted 15 December 2009
Available online 28 December 2009

Keywords:
Cell cycle
Chromatin remodeling
Development
Schimke Immuno-Osseous Dysplasia
smarcal1
Apoptosis

ABSTRACT

Mutations in *SMARCAL1* cause Schimke Immuno-Osseous Dysplasia (SIOD), an autosomal recessive multisystem developmental disease characterized by growth retardation, T-cell deficiency, bone marrow failure, anemia and renal failure. *SMARCAL1* encodes an ATP-driven annealing helicase. However, the biological function of *SMARCAL1* and the molecular basis of SIOD remain largely unclear. In this work, we cloned the zebrafish homologue of the human *SMARCAL1* gene and found that *smarcal1* regulated cell cycle progression. Morpholino knockdown of *smarcal1* in zebrafish recapitulated developmental abnormalities in SIOD patients, including growth retardation, craniofacial abnormality, and haematopoietic and vascular defects. Lack of *smarcal1* caused G0/G1 cell cycle arrest and induced cell apoptosis. Furthermore, using Electrophoretic Mobility Shift Assay and reporter assay, we found that *SMARCAL1* was transcriptionally inhibited by E2F6, an important cell cycle regulator. Over-expression of *E2F6* in zebrafish embryos reduced the expression of *smarcal1* mRNA and induced developmental defects similar to those in *smarcal1* morphants. These results suggest that SIOD may be caused by defects in cell cycle regulation. Our study provides a model of SIOD and reveals its cellular and molecular bases.

Introduction

Schimke Immuno-Osseous Dysplasia (SIOD) is an autosomal recessive multisystem developmental disease characterized by growth failure with short stature, T-cell deficiency with recurrent infection, bone marrow failure, anemia, renal failure, cardiovascular disease, hypertension and stroke in the first decade of the patient's life (Boerkoel et al., 2002; Bokenkamp et al., 2005; Clewing et al., 2007b). SIOD is caused by the mutations in *SMARCAL1* (*s*wi/snf related, *m*atrix associated, *a*ctin-dependent *r*egulator of *c*hromatin, subfamily *a*-*l*ike *1*), which encodes a chromatin remodeling protein (Coleman et al., 2000). However, the function of *SMARCAL1* and the cellular and molecular mechanisms underlying SIOD remain to be elucidated.

SMARCAL1 is homologous to the SWI/SNF chromatin remodeling proteins and the SF2 family of helicases (Boerkoel et al., 2002; Coleman et al., 2000). SWI/SNF family complexes regulate DNA repair, DNA replication, DNA recombination and transcriptional activity through DNA methylation, DNA acetylation, ubiquitination and phosphorylation, consequently regulating cell cycle (Gangaraju and Bartholomew, 2007; Huang et al., 2003; Kadam and Emerson, 2002). SWI/SNF molecules such as excision repair cross-complementation (ERCC), α thalassemia X linked mental retardation (ATRX), brahma-related gene 1 (BRG1) and brahma (BRM) are involved in many developmental processes including cell proliferation, differentiation, apoptosis and homeostasis. Mutations in these genes cause tumorigenesis and human developmental diseases (Cho et al., 2004; Huang et al., 2003; Wang et al., 2007). SMARCAL1 is an ATP-driven annealing helicase (Yusufzai and Kadonaga, 2008), but its cellular function has not been examined. The large number of tissue and organ defects in SIOD patients suggests that SMARCAL1 plays an array of essential roles during development. Clinical studies of SIOD show that patients have normal UV sensitivity and rates of chromosome breakage, indicating no defect in p53-dependent DNA repair following gamma radiation (Boerkoel et al., 2000). However, patients show defects in T-cell proliferation in response to mitogens such as interleukin-2, phytohaemagglutinin and concanavalin A. Anemia patients do not respond to erythropoietin. Patients with bone marrow failure do not respond to stem cell factor and those with growth retardation are not improved with growth hormone supplementation

* Corresponding authors. C. Huang is to be contacted at School of Pharmacy, Shanghai University of Traditional Chinese Medicine, 1200 Cailun Road, Shanghai 201203, China. Fax: +86 21 51322193. J. Du, fax: +86 21 54921735.
E-mail addresses: chuang@sibs.ac.cn (C. Huang), forestdu@ion.ac.cn (J. Du).

0012-1606/$ – see front matter © 2009 Elsevier Inc. All rights reserved.
doi:10.1016/j.ydbio.2009.12.018

(Boerkoel et al., 2000). Those clinical findings imply that SIOD is mainly due to dysfunction in cell proliferation. Besides, some other aspects of SIOD may be related to the defects in cell differentiation, cell survival, cell growth and homeostasis and other developmental processes (Boerkoel et al., 2002; Clewing et al., 2007a; Elizondo et al., 2006), indicating that SMARCAL1 is involved in SIOD through complicated mechanisms.

An animal model greatly facilitates the study of SMARCAL1 functions and the mechanisms underlying SIOD. However deletion of mouse *Smarcal1* and drosophila homologues *Marcal1* do not phenocopy the symptoms of SIOD patients (KS Cho et al., in preparation). The external and rapid development and optical clarity during embryogenesis make zebrafish a powerful vertebrate model for *in vivo* dissecting mechanisms of clinically relevant developmental processes and diseases, particularly hematopoiesis, angiogenesis and T-cell development (Amatruda and Zon, 1999; Dooley and Zon, 2000; Langenau and Zon, 2005; McReynolds et al., 2007), all of which are impaired in SIOD. Gene knockdown by morpholino oligonucleotides (MO) has been demonstrated to be an efficient method of gene targeting during early development of zebrafish (Gamse et al., 2002; Nasevicius and Ekker, 2000).

In the present study, we cloned the zebrafish homologue of the human *SMARCAL1* gene and found that deficiency of zebrafish *smarcal1* caused developmental abnormalities like those found in SIOD patients. Down-regulation of *smarcal1* expression caused cell proliferation defects with the cell cycle arrested at G0/G1 stage, and induced cell apoptosis. Furthermore, we found that *smarcal1* is a direct target of cell cycle regulating transcription factor E2F6. These results shed light on the function of *smarcal1* and the cellular and molecular bases for SIOD.

Materials and methods

Zebrafish strains

AB and Tg (fli1:GFP) zebrafish were obtained from Zebrafish International Resource Center (Eugene, Oregon, USA). Fish were housed in an automatic fish housing system (ESEN, China) at 28 °C.

5′and 3′ RACE

Total RNA was extracted from the adult wild-type (WT) zebrafish head. The TakaRa RACE cDNA amplification kit was used according to the protocol provided by the manufacturer to perform 5′ and 3′ RACE (rapid amplification of cDNA ends). The 5′ RACE primers are outside 5′-ACTTTACCGCGTACTTCAAATG-3′ and inside 5′-GGCATGCGCATTTCAATATA-3′; 3′RACE primers are outside 5′-CCATGCAGACCTCATCCTAGT-3′ and inside 5′-CAAAAGCATTCCCTCCAAA-3′. The RACE products were cloned into pMD18-T vector (TakaRa, Dalian, China) and sequenced.

Morpholinos

Antisense *smarcal1* (ATG-blocking) MO1 TTCTGGAGTCAGACTCACAGACATC, *smarcal1* (splice-blocking) MO2 GCTGAGTCTGTAAAGATGAGCATAA, mdm2 MO CTCTGTTGCCATTTTGGTAGTTATC and *p53* (ATG-blocking) MO GCGCCATTGCTTTGCAAGAATTG (Gene Tools, Philomath, OR, USA) were designed. The standard control MO was used as a control. One nl (8 ng) *smarcal1* MO1, *smarcal1* MO2, *p53* MO, 3 ng of *mdm2* MO or equal amount of control MO was microinjected into each 1-2 cell stage embryo.

RT-PCR

RNeasy Mini kit (QIAgen) was used to isolate total RNA from ten uninjected WT embryos and ten embryos injected with 1 nl MO. After treatment with DNase, 2 μg RNA was reverse-transcribed using Moloney murine leukemia virus (MMLV) Reverse Transcriptase (Promega). TakaRa Taq (TakaRa) was used for PCR for 30 and 26 cycles with *smarcal1* primers and β-*actin* primers, respectively. *Smarcal1* primers for 453 bp product are 5′-TCAAACCTCTGGAAGGGATG-3′ (sense) and 5′-CTCTCTGGAAAGGCATGAGG-3′ (antisense). *Smarcal1* exon1/exon4 primers are 5′-TTGTGTCAGTAAGCGCCTGT-3′ (sense) and 5′-CATCCCTTCCAGAGGTTTGA-3′ (antisense). β-*actin* primers for 559 bp product are 5′-CACCTTCTACAATGAGCTGCGTGTT-3′ (sense) and 5′-GATACCGCAAGATTCCATACCCAAG-3′ (antisense). Human *SMARCAL1* primers are 5′-AGGGGAGACGTAAAGCTGTCC-3′ (sense) and 5′-AGACCATCCAAGCCATCTGC-3′ (antisense). Human β-*ACTIN* primers are 5′-TGGATCAGCAAGCAGGAGTATG-3′ (sense) and 5′-TCAAGAAAGGGTGTAACGCAACT-3′ (antisense).

Real-time RT-PCR

Total RNA from WT and MO injected embryos was extracted using the RNeasy Mini kit (QIAgen, Germany). The amount of reversely transcribed cDNAs was normalized with the real-time ABI 7500 Cycler using β-*actin* as a reference. Primer sequences are listed in Table 1.

Constructs

The full-length human *SMARCAL1*, zebrafish *smarcal1,* zebrafish silent mutation *smarcal1* and *dp1* were cloned into pcDNA3.1 V5/His C by RT-PCR. Zebrafish *smarcal1* 5′UTR-5′cds was cloned into pEGFP-1. Human *SMARCAL1* reporter plasmids were cloned into pGL3. The 453 bp zf *smarcal1* PCR product was cloned into pGEM-T vector for

Table 1
Real-time PCR primer sequences.

Gene	Acc. no.	Forward primer	Reverse primer
β-*actin*	NM_131031	TGACAACGGCTCCGGTATG	TTCTGTCCCATGCCAACCAT
cyclin A2	NM_152949	GCTTTTGGCTTCGAAGTTTGA	TTGTGTACGTGTCGTCAGTGATG
cyclin B1	NM_131513	GCTTATGCCCTGACCCTGAA	GCATCACAGGAACCAGCTCAT
cyclin D1	NM_131025	CAAGCCCTCCCTCCATGAT	GCAACTGTCGGTGCTTTTCAG
cyclin E	NM_130995	GGGCTGAAGTGGTGTGATTTG	GAGCTGCCTGCTTCACGAA
p21	AL912410	TGGAGAAAACCCCAGAGAAGAG	GACGCTTCTTGGCTTGGTAGA
cdkn1b	NM_212792	GTCCGACACCCACATAAACACA	CATCGAAGCGACGACAATGA
cdkn1c	NM_0001002040	GCTCACGGCATTGACTTTTAGA	CGCTCCAGATTGCTTGATACG
gata1	NM_131234	CAGCCACTGGAGGAGTTTACG	TGAATAGAGCGCTGCTGAACTG
beta E1 globin	NM_198073	CATCGTGTACCCCTGGACTCA	GTTTTACCGTGGGCAGCAA
runx1	NM_131603	ACTGGCGCTGCAACAAGAC	TCATCATTTCCCGCCATCA
smarcal1	EU655703	ATCAACTCCAGGACCAAAGCA	TTCTCCTGGGATTTGTTGTGGTA
human *SMARCAL1*	NM_014140.2	CAGCTATGCCGGTCCTAAAGG	GACTGCGATGATCTGCGTGTA
human β-*ACTIN*	NM_001101	GAAGGATTCCTATGTGGGCGA	CATGTCGTCCCAGTTGGTGA

Table 2
Primer sequences used in PCR for constructs.

Construct	5′ primer	3′ primer
pcDNA3.1	*AAGCTT*GATGTCCTTGCCTCTTACAGAGGAG	*GGATCCG*ACAGGGGAGACGTAAAGCTGTCC
h*SMARCAL1*	(*Hin*dIII)	(*Bam*HI)
pcDNA3.1	*GGATCC*AATGTCTGTGAGTCTGACTCC	*GAATTC*CTGGGTCCTGATCCATCAAAG
zf *smarcal1*	(BamHI)	(EcoRI)
pcDNA3.1	*GGATCC***A**ATG**AG**TGTG**TC**TCTGACTCCAGAACAGCAG	*GAATTC*CTGGGTCCTGATCCATCAAAG
zf *silence smarcal1*	(*Bam*HI)[a]	(*Eco*RI)
pcDNA3.1	*GGATCCCC*ATGGCCAAAGATGCTGGTCTGAT	*GTCGAC*GTCCTCGTCGTCGTTTTCATCAAAC
zf *dp1*	(*Bam*HI)	(*Sal*I)
pEGFP	*AAGCTT*CTACCCCTCGCGGTAATGTAAAAAT	*ACCGGT*CGCTGCTGTTCTGGAGTCAGACTCA
zf *smarcal1* 5UTR	(*Hin*dIII)	(*Age*I)
pGL3	*GGTACC*TAACCGTCCACTCGGAAGAC	*AGATCT*CACCTCCAAACTCCCCAGATC
h*SMARCAL1* promoter1	(*Kpn*I)	(*Bgl*II)
pGL3	*GGTACC*GAGTTTGGAGGTGCAGGAGA	*AGATCT*ATGGCGTGACACTTGCTAACAT
h*SMARCAL1* promoter2	(*Kpn*I)	(*Bgl*II)

[a] Bold characters indicate mutated nucleotides.

whole-mount *in situ* hybridization. The primers are listed in Table 2 . *In situ* plasmids of *rag1* and β*E1-globin* were obtained from Dr. R. Patient (Gering and Patient, 2005), and *gata1*, *gata2*, *l-plastin*, *pu.1* and *mpo* plasmids were obtained from Dr. N. Itoh (Yamauchi et al., 2006). *E2F1-5* expression constructs were obtained from Dr. R. Bernards and *E2F6* construct was obtained from Dr. S. Gaubatz.

Whole-mount in situ hybridization (WISH)

WISH was performed as described (Koshida et al., 1998). Digoxigenin (Roche, Mannheim, Germany) labeled cRNA probes were synthesized from linearized plasmids by *in vitro* transcription. Stained embryos were imaged with Olympus SZX9 Zoom Ztereo Microscope (Japan).

Smarcal1 mRNA rescue experiments

The capped full-length *smarcal1*RNA with silent mutations was synthesized using a T7 RNA polymerase and mMessage mMachine high-yield capped RNA transcription kit, according to the manufacturer's protocols (Ambion, Austin TX). For the rescue experiment, each 1–2 cell stage embryo was injected with 200 pg synthesized RNA.

Analysis of cell cycle

To analyze cell proliferation in the zebrafish, embryos were incubated with 10 mM bromodeoxyuridine (BrdU) as described previously (Shepard et al., 2004) and were fixed with 4% paraformaldehyde (PFA). Then whole-mount immunofluorescence was performed with 1:10 anti-BrdU antibody (Roche) and the secondary antibodies conjugated to fluorescein (1:10) according to standard protocols (Shepard et al., 2004). The G2/M phase cells were detected by immunohistochemistry using a rabbit polyclonal anti-phosphorylated histone H3 (pH3) antibody (1:400, Cell Signaling, USA) and 1:500 Alexa red as described previously (Maroon et al., 2002).

Apoptotic cells were determined with the TMR-RED *in situ* cell death detection kit (Roche) as previously described (Liu et al., 2003). The fluorescent signal was visualized and imaged using a Zeiss LSM510 microscope. Z-stack was superimposed using the extended focus feature of Zeiss LSM Image Examiner Version 3.2.0.115 software.

Fluorescence Activated Cell Sorting (FACS) was performed according to a standard protocol (Shepard et al., 2004). Twenty 2 dpf embryos were disaggregated in 500 μl 10% FCS containing DMEM, and the cell suspensions were passed through a 70 μm filter. After being spun at 400*g* for 10 min at 4 °C, liquid was removed. Then cell pellets were re-suspended in 2 ml propidium iodide (PI) solution containing 2 μg RNAase, and incubated in the dark at room temperature for 30 min. Then the cells were immediately analyzed on FACS Calibur (BD, USA).

Alcian blue cartilage staining

Cartilage was stained with Alcian Blue using a modified protocol (Robu et al., 2007). Zebrafish larvae were fixed in 4% PFA, and stained with 0.1% Alcian blue (Sigma) in 70% ethanol and 0.37% hydrochloric acid for overnight at 4 °C. Then embryos were bleached with 3% H_2O_2 and 1% KOH for 4 h.

O-dianisidine staining

For staining of hemoglobin, embryos were treated in freshly prepared O-dianisidine mixture of 2.0 ml o-dianisidine (Sigma, 100 mg/70 ml of ethanol), 0.5 ml of 0.1 M acetate buffer (pH 4.7), 2.0 ml of deionized water, and 0.1 ml of hydrogen peroxide (30%)) for 15 min and then fixed in 4% PFA (Iuchi and Yamamoto, 1983). Embryos were dehydrated in methanol and cleared in 2:1 benzyl benzoate: benzyl alcohol solution (Ransom et al., 1996).

Western blot analysis

Embryos were homogenized in 2× SDS sample buffer and boiled for 5 min. Ten micrograms of protein was separated by 10% SDS-PAGE and transferred to PVDF membrane, blocked for 1 h at room temperature in 5% non-fat dried milk/PBS-T. 1:2000 of anti-V5 (Invitrogen, USA) and HRP-conjugated secondary antibody were incubated with membrane for 1 h at room temperature. The membrane was then washed with PBS-T twice for 10 min each time, incubated with HRP-conjugated secondary antibody for 30 min at room temperature, and washed with PBS-T twice for 10 min. The signals were detected by ECL Plus Western Blotting Detection System according to the manufacturer's specifications (Amersham, Little Chalfont Buckinghamshire, England).

Electrophoretic mobility shift assay (EMSA)

The nuclear protein was extracted from *E2F1-6* and *dp1* co-transfected 293T cells. The sequences of biotin labeled probes are as follows:

Site A 5′-GGCTCTGCAGTCGCGCCTGGGGTCAGGGC-3′
Site B 5′-GGAGTGGGGCGTGGCGCCCGCTTACCTTG-3′
Site C 5′-GGGCGTCCATGGCGGAATGGATTTATGG-3′

EMSA was carried out according to a previous report (MacLachlan and El-Deiry, 2002) using a kit from Pierce (Rockford, IL, USA). Two

hundred times 4 pmol of unlabeled probe was used to confirm the specificity of the binding.

Reporter assay

E2F1-6 and *dp1* expression plasmids were co-transfected with reporter constructs. Transfection efficiencies were normalized by combining 0.5 μg of the relevant plasmids with 0.5 μg of reporter plasmids and 0.1 μg of pREP7 (*Renilla* luciferase) reporter (Huang et al., 2006). All transfections included 1.1 μg of total plasmids and 2 μl Lipofectamine 2000 (Invitrogen, Carlsbad, CA) per 0.5 ml of DMEM. Transfection solution was added to 293T cells for 4 h and then was replaced by culture medium. The cells were harvested for determination of luciferase activity 48 h later using the Dual-Luciferase Reporter Assay System (Promega, Madison, WI). The transfection efficiency was normalized by *Renilla* luciferase activity. All the transfection experiments were performed in triplicate and repeated at least two times.

Phylogenetic tree construction

The phylogenetic tree was constructed by aligning the amino acid sequences of most published Smarcal1 proteins with neighbor-joining (Kumar et al., 2004) and maximum likelihood algorithms (Felsenstein, 2008). The accession numbers of proteins used in the phylogenetic analysis are: *Homo sapiens* NP_054859.2, *Pan troglodytes* XP_516076.2, *Macaca mulatta* XP_001086469.1, *Canis familiaris* XP_536062.2, *Bos Taurus* NP_788839.1, *Rattus norvegicus* NP_001101692.1, *Mus musculus* NP_061287.1, *Xenopus laevis* NP_001089668.1, *Xenopus tropicalis* NP_001072923.1, *Drosophila melanogaster* NP_608883.1, *Caenorhabditis elegans* NP_498401.2.

Statistical analysis

Data analyses were performed using SPSS12.0 for Windows statistical program. All data were presented as means ± SE. Statistical analysis was done by one-way analysis of variance (ANOVA). Differences were considered significant when $P < 0.05$.

Results

Cloning and expression of zebrafish smarcal1

By searching the Ensemble database (http://www.ensembl.org/Danio_rerio/blastview) with amino acid sequences of human SMARCAL1, we obtained one zebrafish *smarcal1* expressed sequenced tag sequence (XM_001334615). We then isolated the full-length complementary DNA from adult zebrafish head cDNA with 5′ and 3′ RACE. A 3083-bp zebrafish *smarcal1* was obtained, in which a poly(A) tailing signal AATAAA is located at the 3′ terminus from nucleotide 3055 to 3060. Zebrafish *smarcal1* cDNA has been deposited in GenBank under the accession no. EU655703.

Using the zebrafish *smarcal1* cDNA sequence to BLAST the Ensemble Zebrafish Genomic Sequence Project database, we found that the gene is located on Chromosome 20. Full-length zebrafish *smarcal1* encodes a putative Smarcal1 protein of 807 amino acids. Sequence similarity comparison indicated that zebrafish putative Smarcal1 protein has 62.2% identity and 78.5% similarity to human SMARCAL1. Zebrafish Smarcal1 has all domains found in mammalian SMARCAL1 proteins (Fig. 1A), including two HepA-related protein (HARP) domains at N-terminus that exhibit single-stranded DNA-dependent ATPase activity, one SNF2 family N-terminal (SNF2_N) domain that involves in transcription regulation, DNA repair, DNA recombination and chromatin unwinding, as well as one helicase superfamily C-terminal (Helicase_C) domain near the C terminus (Supplementary Fig. S1).

A phylogenetic tree was constructed by aligning the amino acid sequences of most published Smarcal1 proteins with neighbor-joining (Kumar et al., 2004) and maximum likelihood algorithms (Felsenstein, 2008). Zebrafish Smarcal1 is conserved within vertebrates (Fig. 1B). Comparison between zebrafish Smarcal1 and its homologues in other species shows that it shares 78.5%, 68%, 69%, 74.4%, and 76.5% similarity to human, mouse, rat, *X. laevis* and *X. tropicalis* Smarcal1, respectively. Taken together, *smarcal1* gene is structurally conserved among zebrafish and mammals.

With use of RT-PCR, *smarcal1* transcript was readily detected through 1-cell stage to the adult (Fig. 1C). Whole-mount *in situ*

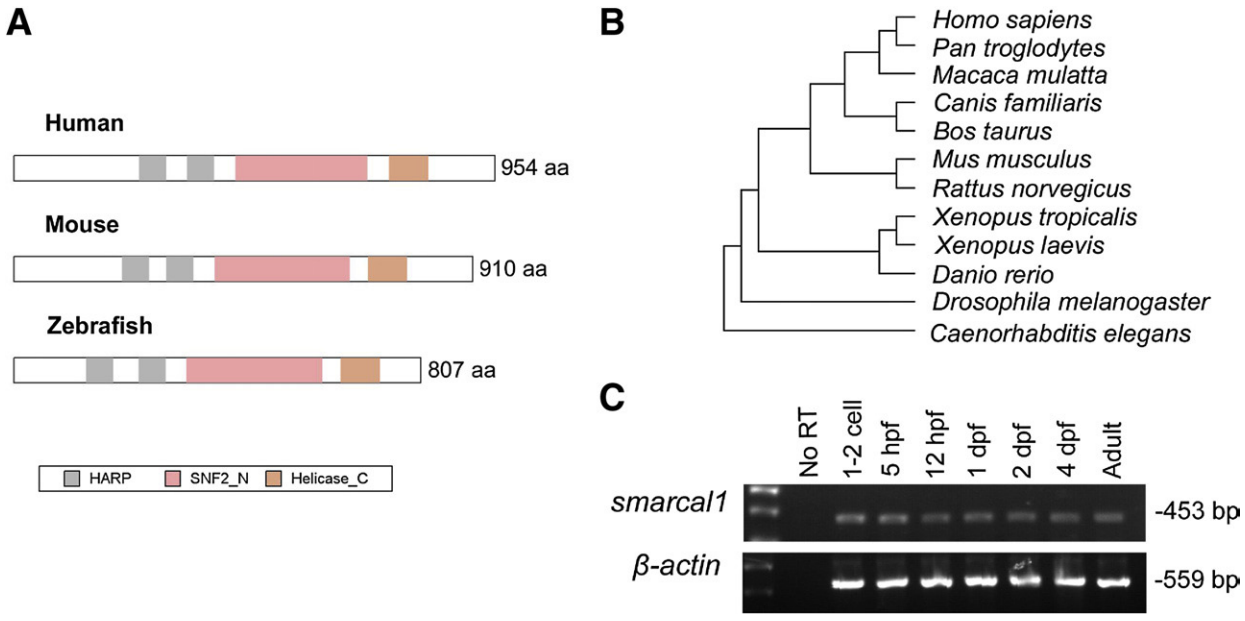

Fig. 1. Structure and expression of *smarcal1*. (A) Structural comparison of putative zebrafish Smarcal1 with human and mouse SMARCAL1 protein. HARP: HepA-related protein; SNF2_N: SNF2 family N-terminal domain; Helicase_C: Helicase superfamily c-terminal domain. (B) Phylogenetic analysis shows that zebrafish Smarcal1 protein is conserved among vertebrates. (C) RT-PCR detection of maternal and zygotic *smarcal1* transcript from 1-cell stage to adult zebrafish.

hybridization (WISH) confirmed the presence of maternal *smarcal1* mRNA at 1-cell stage embryos (Supplementary Fig. S2A). The expression was retained at a high level during blastula and gastrulation, which is at approximately 6 h post-fertilization (hpf) (Supplementary Fig. S2B, C). Around segmentation stages, the *smarcal1* transcript, presumably the zygotic mRNA, appeared in a ubiquitous manner, and was subsequently enriched in the central nervous system (CNS) and eyes as well as the intermediate cell mass (ICM) from the 18-somite stage onwards (Supplementary Fig. S2D, G).

Knockdown of smarcal1 causes abnormal development in zebrafish

To mimic SIOD symptoms, we designed two MOs to knock down zebrafish *smarcal1*. MO1 is against zebrafish *smarcal1* ATG to block smarcal1 protein translation, and MO2 is against intron1 and exon2 junction to block the splice of *smarcal1* mRNA (Fig. 2A). To assay the efficiency of *smarcal1* MO1, we first made an expression construct that links *smarcal1* 5′ UTR and 5′ cds to GFP. Injection of *in vitro* transcribed mRNA into 1–2 cell stage embryos strongly induced GFP signal at 24 hpf (Fig. 2B). However, GFP signal was significantly inhibited by co-injection with *smarcal1* MO1 (Fig. 2B). To further confirm MO1 efficiency, we made an expression construct of full coding region of zebrafish *smarcal1* with V5/His tags. Western blot analysis showed that injection of *in vitro* transcribed mRNA into 1–2 cell stage embryos (200 pg/embryo) efficiently induced Smarcal1 protein at 24 hpf (Fig. 2C). By co-injecting it with *smarcal1* MO1 (8 ng/embryo), the signal was significantly suppressed (Fig. 2C), indicating that MO1 can recognize *smarcal1* mRNA efficiently (Eisen and Smith, 2008). Next, we tested the efficiency of MO2, which was designed to retain exon2. Using primers in exon1 and exon4, a 640 bp band was detected from WT embryos, but a 570-bp product was yielded in the MO2 morphants (Fig. 2D), suggesting MO2 efficiently blocks splicing of *smarcal1* mRNA.

We tested a series of dosages of MO1 (1 ng, 2 ng, 4 ng, 6 ng per embryo) and found no obvious defect in zebrafish gross morphology at the time points we examined (24 hpf, 2 dpf and 4 dpf). Among embryos injected with 8 ng *smarcal1* MO1, we also did not observe obvious gross morphological abnormality during the first 24 h (Figs. 3A–C). However, at 2 days post-fertilization (dpf), developmental defects were readily observed in *smarcal1* MO1 morphants with shorter trunk (32/109, 2.17 ± 0.10 μm compared with 2.59 ± 0.09 μm in control MO injected embryos, $P<0.001$), un-consumed yolk sac (99/109), less dark pigment (105/109) and heart edema (101/109) when compared to wild type (WT) and control MO injected embryos. Examples are shown in Figs. 3D–F and the percentage of embryos affected by the injection is shown inSupplementary Fig. S3B. By 4 dpf, the *smarcal1* morphants had severe gross morphological defects (data not shown). We observed death in part of *smarcal1* morphants (death 70/99). The rest of the morphants (growth delayed) could not hatch (26/29), and displayed heart edema (28/29) and shorter trunk and smaller head and eyes (23/29). Also, when compared to the heart rate of the control MO injected embryos (128.9 ± 6.5 times/min,Supplementary movie 1), the morphants exhibited lower heart rates (24/29, 59.2 ± 20.2 times/min,Supplementary movie 2).

In order to confirm MO1 specificity, we then tested MO2 effects. We found that like MO1, MO2 did not cause abnormal development at 24 hpf but led similar phenotypes at 2 dpf (Supplementary Fig. S3A, B). To further rule out the non-specific effects of *smarcal1* MOs, we introduced five-nucleotide silent mutations into the full-length zebrafish *smarcal1* mRNA (Eisen and Smith, 2008). The primers are shown in Table 2. Injection of 200 pg silent *smarcal1* mRNA alone did not cause phenotype in embryos (data not shown). We co-injected 200 pg of this mRNA with *smarcal1* MO1 and found that the developmental defects mentioned above were largely corrected (Supplementary Fig. S3A, B). Similarly, co-injection of *smarcal1* mRNA and MO2 partially rescued the defects in MO2 morphants

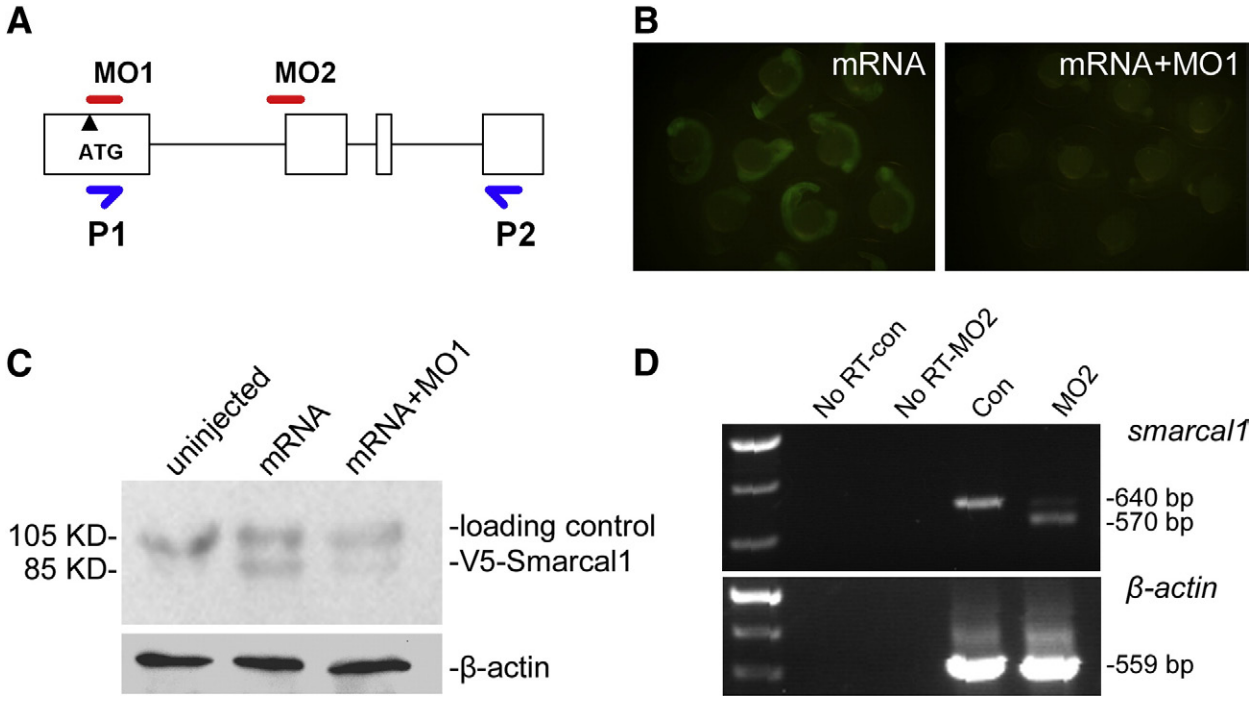

Fig. 2. Design and efficiency of *smarcal1* MOs. (A) Design of *smarcal1* MOs and RT-PCR primers for detecting the splice-blocked *smarcal1* mRNA. P1 and P2 indicate the primers used in (D). (B) Embryos with injection of *smarcal1* 5′ UTR-5′cds-GFP mRNA (50 pg per embryo) displayed green fluorescence, whereas co-injection of *smarcal1* MO1 (8 ng per embryo) with 5′ UTR-5′cds-GFP mRNA (50 pg per embryo) blocked fluorescence signal. (C) Knockdown efficiency of *smarca11* MO1 analyzed by Western blot with V5 antibody. V5-tagged full-length zebrafish *smarcal1* injected embryos (200 pg per embryo) showed the induction of 85 KD protein, whereas co-injection with 8 ng of MO1 inhibited the protein translation. A 105 KD non-specific band and β-actin serve as loading control. (D) RT-PCR analysis of splice-blocking efficiency of MO2. A 640 bp product was amplified from WT embryos and MO2 deleted about 70 nucleotides of *smarcal1* mRNA. In each group, 20 embryos were pooled for western blot and RT-PCR experiments.

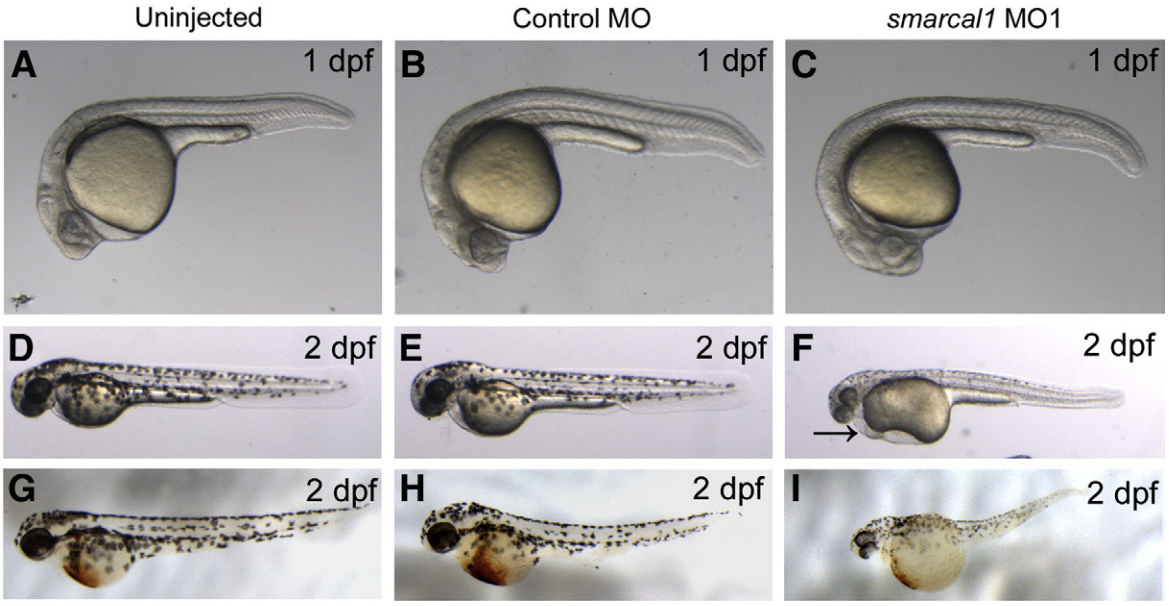

Fig. 3. Knockdown of *smarcal1* causes developmental defects in zebrafish. (A–F) The gross morphology of 1 dpf and 2 dpf *smarcal1* morphants. The morphology of uninjected and control MO injected embryos (8 ng per embryo) was largely normal. By 2 dpf, the embryos injected with *smarcal1* MO (8 ng per embryo) showed growth defects including less dark pigment, unconsumed yolk sac and heart edema (F). (G–I) O-dianisidine staining of 2 dpf embryos showed reduced hemoglobin-positive cells on the yolk in *smarcal1* morphants (I). Anterior is to the left.

(Supplementary Fig. S3B). These results confirmed the specificity of *smarcal1* MOs.

Alcian blue staining revealed that cartilage developed normally in WT and control MO injected zebrafish larvae at 5 dpf (Supplementary Fig. S4A–D). In contrast, severely reduced growth of pharyngeal cartilage was found in *smarcal1* morphants (Supplementary Fig. S4E, F). The ceratobranchials 3–5 were absent, whereas the sizes of the dorsal hyosymplectic cartilage, the ventral ceratohyal and the jaw palatoquadrate were reduced (Supplementary Fig. S4E, F), suggesting that the maturation of arch cartilage requires *smarcal1*.

SIOD patients suffer migraine, cerebral ischaemia and transient ischemic attacks, all of which may be the result of arteriosclerosis in the first decade of life, suggesting defects in blood vessel formation and/or maintenance. We then examined whether knockdown of *smarcal1* causes developmental defects in vasculogenesis and/or angiogenesis. At 2 dpf zebrafish embryos, the intact dorsal aorta and axial circulation were observed in *smarcal1* morphants (data not shown), suggesting that the *smarcal1* is not essential for vasculogenesis. The formation of the parachordal vessel (PAV) and sub-intestinal vessel (SIV) is a process of angiogenesis (Isogai et al., 2003; Nicoli and Presta, 2007). Microangiography showed that both PAV and SIV were sprouted normally at uninjected and control MO embryos, whereas they were absent in *smarcal1* morphants (19/20) at 3 dpf (Supplementary Fig. S4G–I), suggesting that *smarcal1* is required for angiogenesis.

Knockdown of smarcal1 impairs hematopoietic development

Using O-dianisidine staining, we found that there were fewer red blood cells in *smarcal1* morphants at 2 dpf (35/40) (Fig. 3I) compared to uninjected (Fig. 3G) and control MO injected embryos (Fig. 3H), suggesting an impaired erythrogenesis caused by knockdown of *smarcal1*.

To address effects of *smarcal1* on hematopoiesis, WISH was performed to examine the expression of blood markers in *smarcal1* morphants. The expression of *scl* and *gata2*, the hemangioblast and hematopoietic stem cell markers (Amatruda and Zon, 1999; Patterson et al., 2007; Yamauchi et al., 2006), respectively, remained intact in *smarcal1* morphants (Figs. 4A, B, and E, F), indicating that *smarcal1* is not required for proliferation of hemangioblasts and hematopoietic stem cells. Although the initiation of primitive erythropoiesis is normal, the expression of *gata1*, that determines the fate of erythroid progenitor cells (Amatruda and Zon, 1999), was markedly reduced in *smarcal1* morphants (28/30, Figs. 4C, G). Consistently, the expression of mature erythrocyte marker *βE1-globin* was also reduced (32/33, Figs. 4D, H). Real-time RT-PCR confirmed that *gata1* and *βE1-globin* mRNA levels were significantly reduced at 24 hpf *smarcal1* morphant (Fig. 4I). These results indicate that deficiency of *smarcal1* causes abnormal proliferation and/or differentiation of erythroid progenitors. To test whether the primitive myelopoiesis is impaired in *smarcal1* morphants, the myeloid markers were assayed in 18 hpf embryos. The expressions of myeloid progenitor marker *pu.1*, monocyte/macrophage marker *l-plastin* and granulocyte marker *mpo* (Bennett et al., 2001) were generally normal (Figs. 4J, O), indicating that *smarcal1* is not required for the primitive myelopoiesis.

Next, we examined whether deficiency of *smarcal1* affects definitive hematopoiesis. RT-PCR results showed that the expression of definitive hematopoietic marker *runx1* (Kalev-Zylinska et al., 2002; Lam et al., 2009) was suppressed by *smarcal1* knockdown at 24 hpf embryos (Fig. 4P). WISH showed the expression of *rag1*, a thymic marker (Langenau and Zon, 2005), was reduced (23/25, data not shown), suggesting the loss of the thymocytes in *smarcal1* morphants. The defects in definitive myelopoiesis were examined at 30 hpf embryos. The expressions of *pu.1* (38/40, Figs. 4Q, T), *l-plastin* (37/37, Figs. 4R, U) and *mpo* (32/36, Figs. 4S, V) were suppressed at ICM of 30 hpf *smarcal1* morphants.

Knockdown of smarcal1 reduces cell proliferation and induces apoptosis

The development of the organisms depends on the balance between cell proliferation and apoptosis. Based on many lines of SIOD clinical evidence, we hypothesized that *smarcal1* is involved in the cell cycle regulation. To examine cell proliferation changes in *smarcal1* deficient embryos, we incorporated the S-phase marker of cell cycle BrdU into the DNA of embryos and found that the number of BrdU-positive nuclei in 20 hpf *smarcal1* morphants were largely reduced (Figs. 5A, B, E, F), even though there was no gross morphology

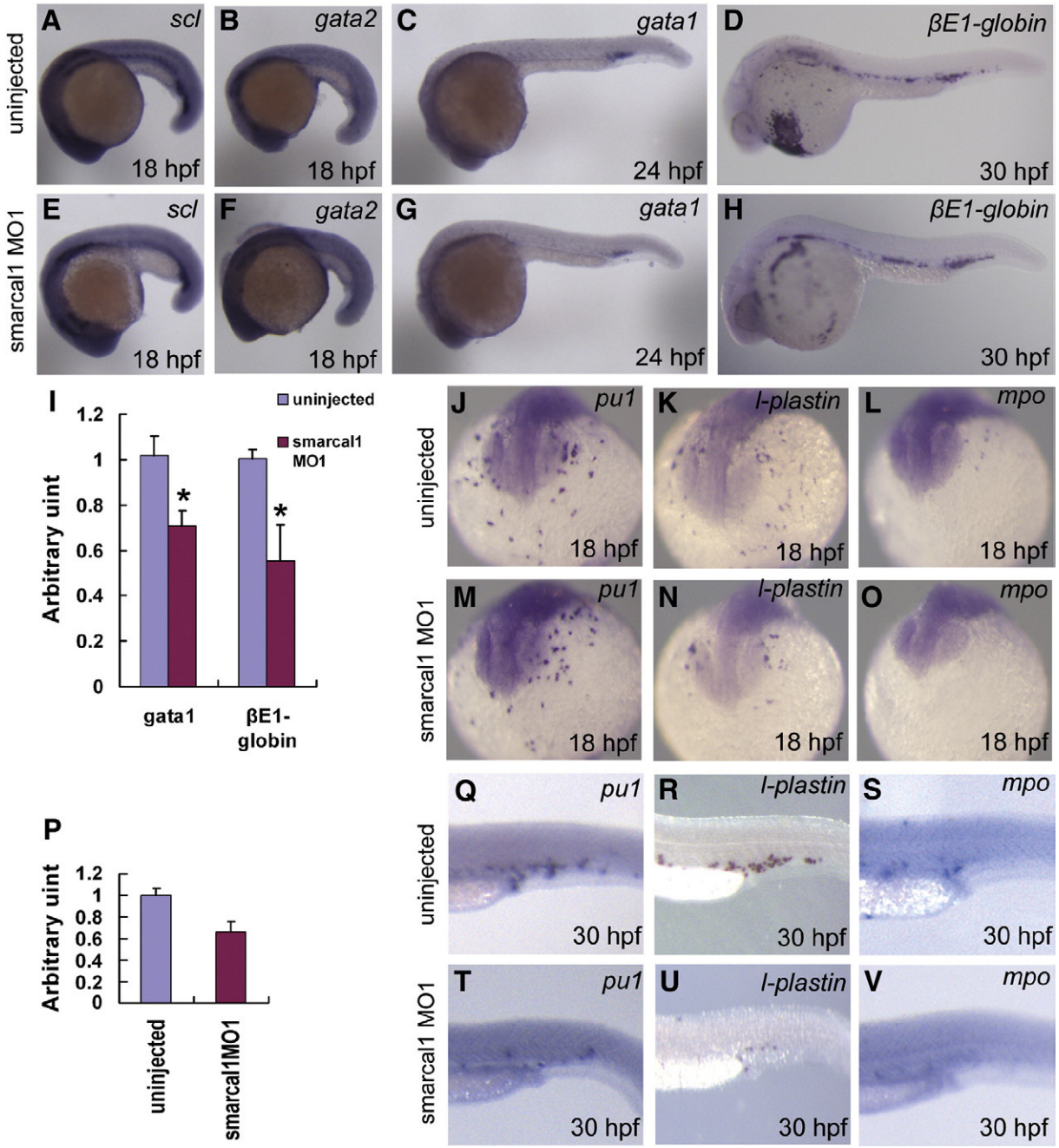

Fig. 4. Knockdown of *smarcal1* reduces expression of hematopoietic genes. (A–H) WISH shows that expression of hemangioblast marker *scl* and hematopoietic stem cell marker *gata2* were not affected by knockdown of *smarcal1*, whereas erythroid progenitor marker *gata1* and erythroid marker β-*E1 globin* were significantly reduced. All embryos are in lateral view with anterior to the left. (I) Real-time RT-PCR results from 24 hpf embryos show that *smarcal1* MO significantly reduced the expression of *gata1* and β-*E1 globin.* (J–O) The expressions of myeloid progenitor marker *pu.1*, macrophage marker *l-plastin* and heterophil granulocyte marker *mpo* were not obviously changed by knockdown of *smarcal1* at 18 hpf. (P) Real-time RT-PCR shows reduced expression of definitive erythroid marker *runx1* in 24 hpf MO1 injected embryos. (Q–V) Knockdown of *smarcal1* suppressed definitive hematopoiesis.. (Q–S) show the expression of *pu.1*, *l-plastin* and *mpo* at definitive myeloid cells and (T–V) show the markers were down-regulated by knockdown of *smarcal1* at 30 hpf. The real time PCR results were obtained from at least three experiments. β-*actin* mRNA was measured as an internal control. Data are presented as means ± SE. **P*< 0.05.

change at this time point (see Fig. 3C). By 2 dpf, a significant reduction of BrdU-positive nuclei was also observed in the head, eyes, yolk sac, ICM and tail in *smarcal1* morphants (Figs. 5C, D, G, H). The quantification of BrdU-positive nuclei in 2 dpf embryo head is shown at Fig. 5I. We further examined changes in the number of G2/M phase cells using immunostaining of phosphorylated histone 3 (pH3), which is phosphorylated in G2/M and is dephosphorylated in anaphase (Hendzel et al., 1997). As we found in BrdU staining, the numbers of pH3-positive cells were also significantly reduced by knockdown of *smarcal1* at both 20 hpf and 2 dpf embryos (Figs. 5J, Q). The quantification of pH3-positive nuclei in 2 dpf embryo head is shown in Fig. 5R. To assay the cell cycle, DNA content of the cells from 2 dpf embryos was analyzed by Fluorescence Activated Cell Sorting (FACS). Propidium iodide (PI) staining showed that uninjected and control MO embryos displayed 62% and 60% of cells at G0/G1, 15% and 16% at S, and 23% and 23% at G2/M phase, respectively, whereas the *smarcal1* morphants exhibited cell accumulation at G0/G1 phase (91%) and reduction at both S (5%) and G2/M (4%) phase (Fig. 5S). These results indicate that cell cycle was arrested at G0/G1 phase in *smarcal1* morphants.

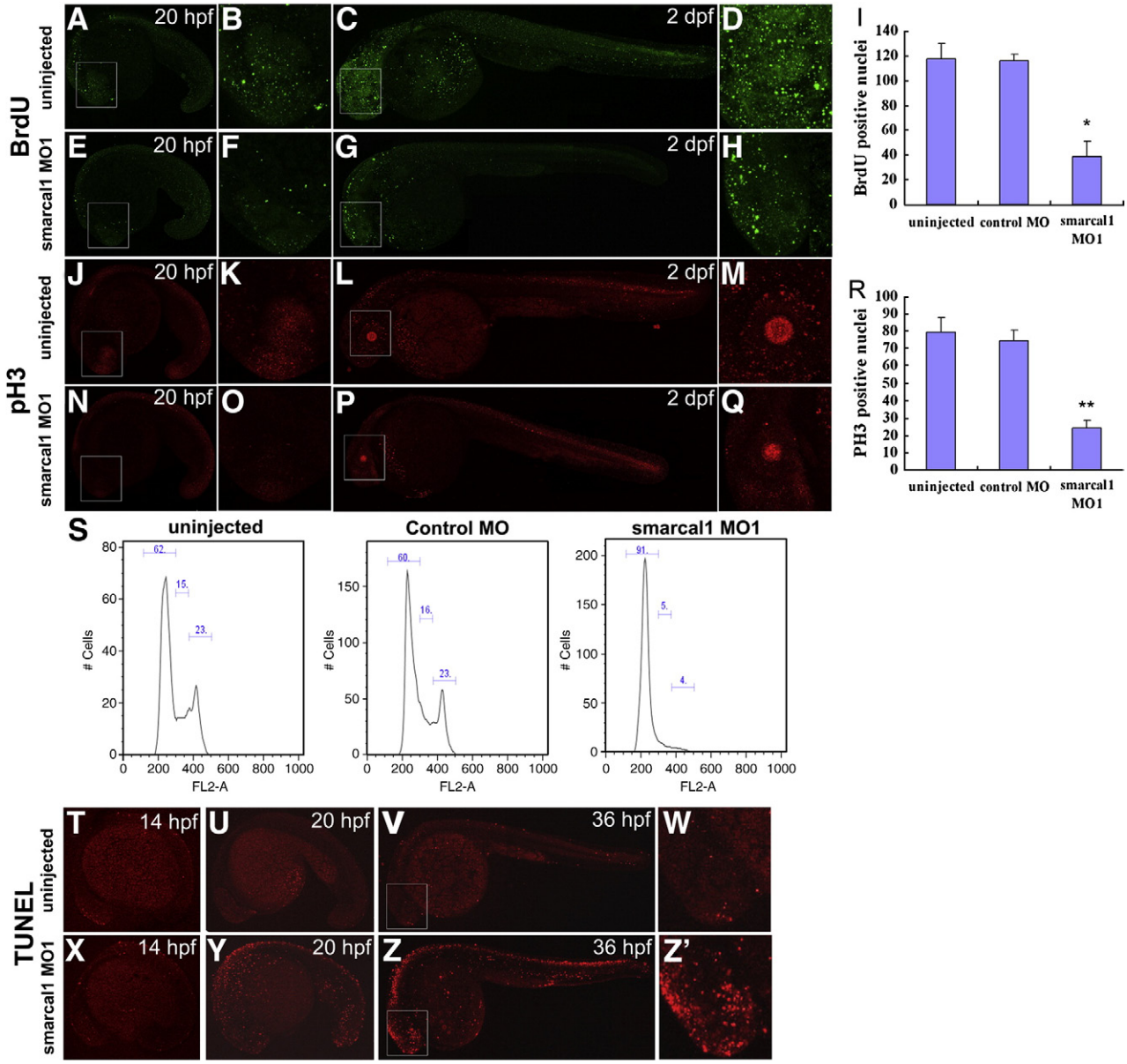

Fig. 5. Knockdown of *smarcal1* disrupts the cell cycle. (A–H) Confocal images of whole-mount immunostaining of BrdU show S-phase cells. (B, D, F, H) are higher magnification of the boxed regions in (A, C, E, G), respectively, which indicate BrdU-positive nuclei in the head. (I) The quantification of BrdU-positive nuclei in the head of uninjected, control MO and *smarcal1* MO1 embryos at 2 dpf. The data was counted from three individual embryos. *$P<0.05$. (J–Q) Confocal images of whole-mount immunostaining of pH3 show G2/M phase cells. (K, M, O, Q) are higher magnification of the boxed regions of (J, L, N, P), respectively, which indicate pH3-positive nuclei in the head. (R) The quantification of pH3-positive nuclei in the head of uninjected, control MO and *smarcal1* MO1 embryos at 2 dpf. The data was counted from three individual embryos. **$P<0.01$. regions of S. (S) FACS analysis with PI staining of DNA contents shows that uninjected and control MO injected embryos had normal cell cycle, whereas the *smarcal1* morphants showed cell accumulation at G0/G1 phase and cell reduction of S and G2/M phase at 2 dpf. (T–Z') Apoptosis analysis with TUNEL staining of *smarcal1* morphants at 14 hpf (T, X), 20 hpf (U, Y) and 36 hpf (V, Z). (W, Z') are higher magnification of the boxed regions in (V) and (Z), respectively. All experiments were repeated at least three times.

To examine whether the deficiency of *smarcal1* causes apoptosis, TUNEL was used to detect apoptotic cells in zebrafish embryos. While the number of TUNEL positive cells in 14 hpf embryos remained unchanged (Figs. 5T, X), it was significantly increased in 20 hpf *smarcal1* morphants (Figs. 5U, Y), even though there was no obvious abnormality of gross morphology at this time point (see Fig. 3C). By 36 hpf, the number of positive cells was dramatically increased in the brain, eyes, trunk, tail and ICM (Figs. 5V, W, Z, Z'), suggesting that the developmental defects of *smarcal1* morphants may be partially caused by the increase of apoptosis.

The cell cycle transition depends on the function of CDK-cyclin complexes. To explore whether deficiency of *smarcal1* causes changes in the expression of cell cycle genes, we assayed the expression of a group of *cyclins* by real-time RT-PCR. We found that mRNA levels of *cyclinA2*, that promotes G1 to S phase transition (Lehner and O'Farrell, 1989; Sprenger et al., 1997), were reduced significantly in both 1 dpf and 2 dpf *smarcal1* morphants (Fig. 6A). The expression levels of *cyclinB1*, *cyclinD1* and *cyclinE* were not altered markedly at 1 dpf, but the mRNA levels of *cyclinD1* were increased at 2 dpf morphants. These results are consistent with reduction of BrdU-positive cells in *smarcal1* morphants (Fig. 5I). The cell cycle is also negatively regulated by cyclin-dependent kinase inhibitor proteins (kips/cips) p21cip1 (p21), p27kip1 (cdkn1b) and p57kip2 (cdkn1c), all of which are expressed at G1 phase (Vidal and Koff, 2000). It is known that *p21cip1* inhibits the cell cycle transition from G1 to S phase and controls the cell cycle exit to G0. We found that *p21* mRNA level was greatly increased at 1 dpf and 2 dpf embryos by knockdown of *smarcal1* (Fig. 6B), whereas *p27kip1* and

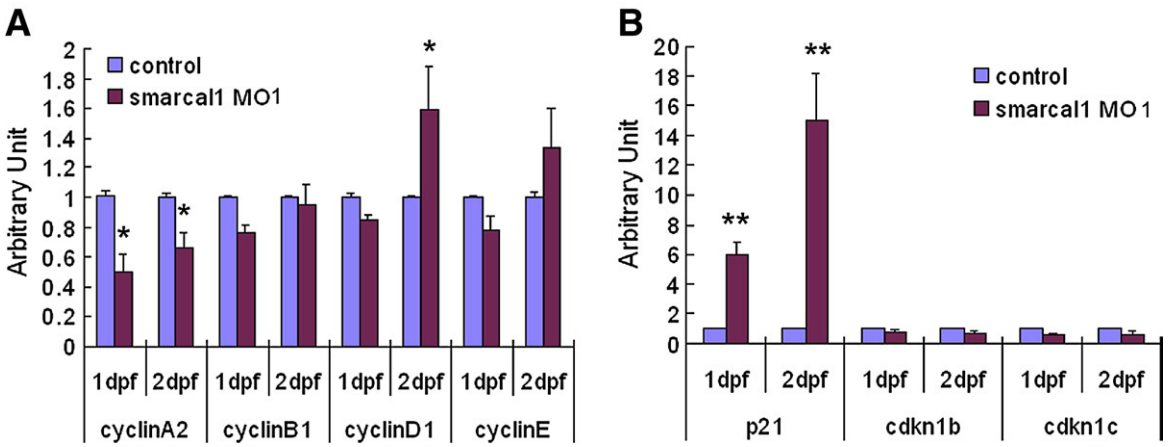

Fig. 6. Knockdown of *smarcal1* changes the expressions of cell cycle-related genes. Real-time PCR experiments show that mRNA levels of *cyclinA* (A) was suppressed and *p21* (B) was increased by *smarcal1* MO at 1 dpf and 2 dpf. The levels of *cyclinB1*, *cyclinD1*, *cyclinE* were not changed at 1 dpf, whereas the expressions of *cyclinD1* increased at 2 dpf (A). The expression levels of *cdkn1b (p27)* and *cdkn1c (p57)* remained no significant change (B). The results were obtained from at least three experiments. β-*actin* mRNA was measured as an internal control. Data are presented as means ± SE. **P*< 0.05; ***P*< 0.01.

p57kip2 expressions were not significantly changed (Fig. 6B). Collectively, our data imply that G0/G1 phase arrest in *smarcal1* morphants may be caused by reduced expression of *cyclinA2* and increased expression of *p21*.

Previous studies suggested that 15–20% of MOs used in zebrafish can induce neural death at 24 hpf or earlier stages through the activation of *p53* signaling (Ekker and Larson, 2001; Robu et al., 2007). Co-injection with *p53* MO could rescue the neural death caused by those MOs (Bill et al., 2008; Gongal and Waskiewicz, 2008; Jia et al., 2008; Robu et al., 2007). Thus we co-injected *p53* MO with *smarcal1* MO to exclude the possibility that *smarcal1* MO may have such off-targeting effects on *p53* signaling. We observed that knockdown of *p53* did not cause obvious developmental defects (data not shown), consistent with that *p53* mutations did not affect the embryonic development in zebrafish (Berghmans et al., 2005). We found that the gross morphology, erythrogenesis and apoptosis of co-injected embryos were not obviously changed when compared to *smarcal1* morphants (Supplementary Fig 5). To test the efficiency of *p53* MO, we injected 3 ng of *mdm2* MO and found that *mdm2* MO caused early apoptosis in 24 hpf zebrafish embryos (Supplementary Fig 3C), consistent with a previous report (Robu et al., 2007). Co-injection of *p53* MO significantly reduced apoptosis induced by *mdm2* MO (Supplementary Fig 3C), indicating *p53* MO effectively inhibits p53 signaling, the abnormalities observed in *smarcal1* morphants are not due to the *p53* signaling activation, and the apoptosis in *smarcal1* morphants may be *p53*-independent.

SMARCAL1 is down-regulated by E2F6

The involvement of *smarcal1* in cell cycle regulation prompted us to investigate the association between *smarcal1* and *E2F6*, a cell cycle regulating transcription factor. We used S_Site 1.0 (http://compel.bionet.nsc.ru/FunSite/SiteScan.html) to search for E2F binding sites at *SMARCAL1* promoter. At human *SMARCAL1* promoter, a 869 bp CpG island, usually associated with gene promoter and found at almost all house-keeping genes (Cho and Hedrick, 1997), was identified between −933 to −1801. Three putative E2F binding sites were found between −1250 to −1261 (site A), −1069 to −1080 (site B) and −965 to −976 (site C), respectively. In zebrafish, four e2f binding sites were found (Supplementary Fig. S6). To investigate whether E2Fs bind to these sites, EMSA was performed with use of biotin labeled E2F binding probes and nuclear protein extracts from *E2F1-6* and *dp1* co-transfected 293T cells. While E2Fs were not found to bind with site B and site C (data not shown), E2F6 but not E2F1-5 bound to site A (Fig. 7A). This binding was completely reduced by unlabeled probes (Fig. 7A). The results suggest that *SMARCAL1* is a direct target of E2F6.

To test whether E2F6 activates or suppresses *SMARCAL1* transcription, *SMARCAL1* promoter sequence containing E2F binding sites (P1) was cloned into pGL3 vector, and the luciferase reporter assay was carried out. We found that E2F6 significantly suppressed *SMARCAL1* transactivity by over-expression of E2F6 (Fig. 7B). In contrast, transactivity of *SMARCAL1* promoter sequence without E2F binding sites (P2) was not altered (Fig. 7B). To validate this point, *SMARCAL1* mRNA level was examined in *E2F6* transfected 293T cells by RT-PCR. Over-expression of *E2F6* decreased *SMARCAL1* expression (Figs. 7C, D). These results indicate that E2F6 is a transcriptional suppressor of *SMARCAL1*.

To further address whether *E2F6* inhibits *smarcal1* expression *in vivo*, we injected *E2F6* mRNA into 1–2 cell zebrafish embryos. *E2F6* mRNA injection significantly disrupted zebrafish development with phenotypes similar to those observed in *smarcal1* morphants (Figs. 7E, F). Consistently, *smarcal1* transcription level was markedly inhibited in *E2F6* mRNA injected embryos at 1 dpf (Figs. 7G, H). These results suggest that *smarcal1* may play important roles downstream to E2F6 in cell cycle regulation.

Discussion

Smarcal1 loss of function in zebrafish resembles SIOD symptoms

In this work, we first identified a zebrafish structural and functional homologue of the human *SMARCAL1* gene. Structural analysis showed that the zebrafish *smarcal1* shares 78.5% and 68% similarity to human and mouse homologues, respectively. This high degree of sequence similarity indicates functional conservation. Similar to its human and mouse counterparts (Boerkoel et al., 2002; Elizondo et al., 2006), zebrafish *smarcal1* is expressed ubiquitously at embryonic stages, implying a wide range of functions of *smarcal1* during development.

SIOD patients have multiple developmental defects such as growth retardation, lymphopenia, bone marrow failure, anemia, neutropenia, craniofacial abnormality, renal failure and premature death in their first decades of life. An animal model is fundamentally important for understanding the cellular and molecular bases of SIOD and functions of *SMARCAL1*. In the present work, we found that knockdown of *smarcal1* in zebrafish caused multi-system developmental defects, including growth retardation, craniofacial abnormality, reduced thymic development, and defects in both primitive and definitive hematopoiesis and angiogenesis. SIOD is considered a postnatal

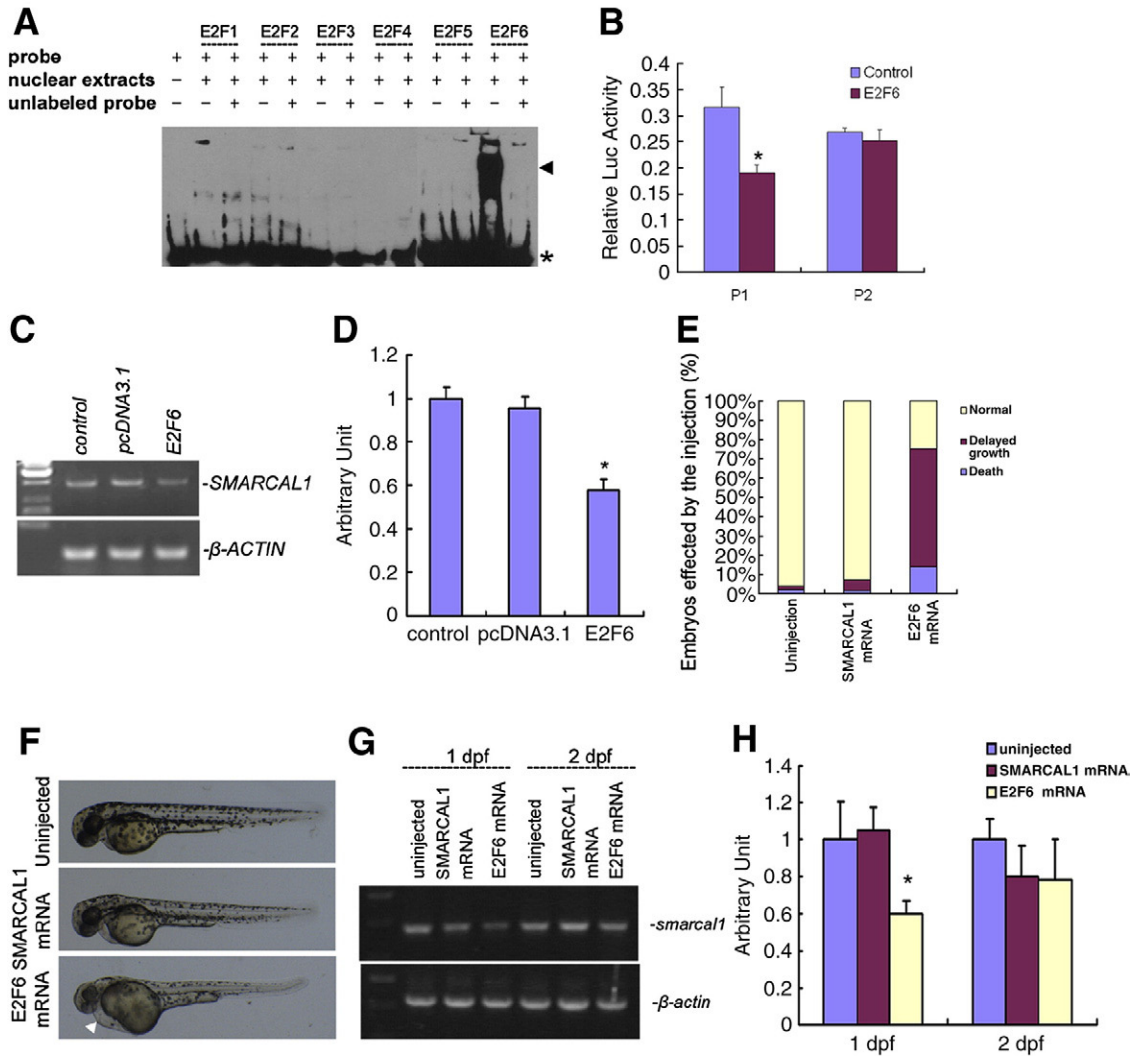

Fig. 7. *smarcal1* is a direct target of E2F6. (A) Demonstration of E2Fs binding to *SMARCAL1* promoter by EMSA. EMSA using nuclear protein extracts from *E2Fs-dp1* co-transfected 293T cells shows that *E2F-dp1* complexes bound to E2F sites in *SMARCAL1* promoter. 200 times unlabeled probe was used to compete with the biotin labeled probe. The black arrowhead indicates the band of specific DNA–protein complexes. The asterisk indicates the band of the unbound probe. (B) Reporter gene assay shows *SMARCAL1* transactivity was specifically inhibited by E2F6. *E2F6-dp1* co-transfected with *SMARCAL1* reporter plasmids and renilla luciferase activity was measured as transfection control. P1: pGL3-*SMARCAL1* promoter1 containing E2F binding sites. P2: pGL3-*SMARCAL1* promoter2 without E2F binding sites.*$P<0.05$. (C) RT-PCR analysis of *SMARCAL1* expression in *E2F6* transfected 293T cells. The empty vector of pcDNA3.1 was transfected as a control. PCR was performed for 26 cycles. (D) Real time PCR analysis of mRNA levels in 293T cells in (C). The results represent three experiments. β-*actin* mRNA was measured as an internal control. Data are presented as means ± SE. *$P<0.05$. (E) Embryos injected with *E2F6* mRNA (200 pg per embryo) showed gross morphology defects similar to *smarcal1* morphants at 2 dpf. Human *SMARCAL1* mRNA (200 pg per embryo) was used as control. (F) Example of *E2F6* mRNA injected embryos. White arrowhead in the bottom image indicates the heart edema. (G) *E2F6* mRNA injection inhibits *smarcal1* mRNA expression in zebrafish embryos at 24 hpf but not at 48 hpf. Human *SMARCAL1* mRNA (200 pg per embryo) was used as control. (H) Real time PCR analysis of mRNA levels in embryos in (G). The results represent three experiments. β-actin mRNA was measured as an internal control. Data are presented as means ± SE. *$P<0.05$.

developmental disease (Boerkoel et al., 2002), though *SMARCAL1* is expressed in all tissues at high levels in very early stages of human embryonic development (Deguchi et al., 2008). Similarly, zebrafish *smarcal1* transcript is expressed ubiquitously in the zebrafish embryos from the 1-cell stage, but gross morphological abnormalities caused by knockdown of *smarcal1* were only observed after 24 hpf. It indicates that knockdown of *smarcal1* in zebrafish can recapitulate SIOD symptoms.

We provided several lines of evidence to demonstrate the specificity of *smarcal1* MOs. First, two MOs designed to block the translation and splicing of *smarcal1*, respectively, led to similar phenotypes. In contrast, embryos injected with a standard control MO developed normally. Second, the two MOs could efficiently knock down *smarcal1* (see Fig. 2). Third, full-length *smarcal1* with silent mutations largely rescued the phenotypes of MO1 and partially rescued the phenotypes of MO2 (seeSupplementary Fig. S3B). Taken together, zebrafish *smarcal1* morphant can serve as an animal model to study the cellular and molecular mechanisms underlying SIOD.

Smarcal1 is required for hematopoiesis

In this work, we showed that impaired hematopoiesis is one of the major defects induced by *smarcal1* deficiency. Previous studies have shown that chromatin remodeling molecules play important roles in the hematopoietic stem cell self-renewal, multilineage differentiation (Horsfield et al., 2007; Yoshida et al., 2008), primitive and definitive *alpha*-and *beta-globin* transcription, primitive erythrocyte apoptosis (Griffin et al., 2008) and T-cell differentiation (Sawalha, 2008), indicating that chromatin remodeling molecules are important regulators in hematopoiesis. We demonstrated a link between *smarcal1* and hematopoiesis during zebrafish development. We found that the expressions of *gata1*, *beta-E1 globin* and *runx1* in *smarcal1* morphants were suppressed, indicating abnormal proliferation of

both primitive and definitive erythroid progenitors. Similarly, *smarcal1* is required for the proliferation of definitive myeloid cells and lymphocyte since the expressions of *pu.1*, *l-plastin* and *mpo* and *rag1* were decreased by knockdown of *smarcal1*. Our results are consistent with the findings that SWI/SNF molecules play crucial roles in a wide variety of developmental processes during hematopoiesis via gene transcription regulation.

Smarcal1 is required for cell cycle progress

SMARCAL1 encodes an ATPase-dependent chromatin remodeling molecule that contains all functional domains of SWI/SNF members. SWI/SNF family chromatin remodeling complexes promote or inhibit the transcriptional activity and are involved in cell cycle regulation through DNA methylation, acetylation, ubiqulation and phosphorylation, DNA repair, DNA replication and DNA recombination (Gangaraju and Bartholomew, 2007; Huang et al., 2003; Kadam and Emerson, 2002). Recent study has shown that SMARCAL1 has DNA annealing helicase activity (Yusufzai and Kadonaga, 2008) that may contribute to the helicity of DNA at gene promoters. DNA superhelicity is a major regulator of gene expression in bacteria (Cheung et al., 2003; Dai and Rothman-Denes, 1999; Salmon et al., 2003). Changing the level of DNA superhelicity could enhance or inhibit gene expression (Lim et al., 2003). Deficiency of *smarcal1* may result either in inappropriate or suppressed gene expression linked to the cell cycle. It implies that SIOD symptoms may be due to cell cycle defects caused by loss of *SMARCAL1*.

Our main finding is the demonstration of involvement of *smarcal1* in cell cycle regulation. First, the cell cycle S phase marker BrdU incorporation and G2/M phase marker phosphorylated histone-3 signal were significantly reduced in *smarcal1* morphants. Meanwhile, FACS experiments showed that the cell cycle was arrested at G0/G1 phase, indicating that deficiency of *smarcal1* causes defects in G1/S phase transition. Second, the expression of the cell cycle molecule *cyclinA2*, which promotes G1 to S phase transition (Lehner and O'Farrell, 1989; Sprenger et al., 1997), was suppressed, while CDK inhibitor A (*p21*), which is an inhibitor of G1 to S transition (Vidal and Koff, 2000), was up-regulated. This indicates that *smarcal1* modulates the cell cycle through transcriptional regulation similar to other SWI/SNF family members (Gangaraju and Bartholomew, 2007; Kadam and Emerson, 2002). Finally, *smarcal1* morphants exhibit p53 independent cell death, suggesting the developmental defects of *smarcal1* morphants may be partially caused by excessive apoptosis. Thus *smarcal1* is required for cell cycle check point transition, which may be the cellular basis of SIOD.

Smarcal1 is a direct target of E2F6

E2F transcription factors regulate the expression of genes essential for the cell cycle transition, DNA replication, DNA synthesis, DNA repair and mitosis, and thus play crucial roles in cell proliferation, differentiation and apoptosis (DeGregori and Johnson, 2006; Korenjak and Brehm, 2005; Wu et al., 2001). Deletion of *E2Fs* causes hematopoietic progenitor and immune cell deficiency by disruption of the cell cycle, resulting in anemia and leucopenia (Gabellini et al., 2006; Korenjak and Brehm, 2005). E2F1-5 serve as both transcriptional activators and suppressors, whereas E2F6 suppresses E2F-responsive genes (Ogawa et al., 2002; Trimarchi et al., 1998). Our data demonstrate that *smarcal1* is a direct target of E2F6. First, the EMSA experiment showed E2F6 protein specifically bound to E2F site in *SMARCAL1* promoter, and this binding could be inhibited completely by an unlabelled probe. Second, reporter gene analysis confirmed that *SMARCAL1* was suppressed by over-expression of E2F6 both *in vitro* and *in vivo*. Third, over-expression of *E2F6* reduced transcription levels of *SMARCAL1* both *in vivo* and *in vitro*. These results further support that *smarcal1* is a cell cycle regulator.

In summary, we cloned the zebrafish homologue of human *SMARCAL1* gene and found that *smarcal1* loss of function recapitulated the symptoms of SIOD patients with respect to growth retardation, blood cell deficiency, craniofacial abnormality and angiogenesis defect. It indicates that zebrafish can serve as an animal model for studying the mechanism of SIOD. Furthermore, we demonstrated that *smarcal1* is involved in cell cycle regulation during development. Taken together, our study indicates that SIOD may be caused by cell proliferation defects and excessive apoptosis resulting from *SMARCAL1* mutations.

Acknowledgments

We thank Drs. M.M. Poo and Q. Zhai of Shanghai Institutes for Biological Sciences, Chinese Academy of Sciences for critical reading and comments, G. Cui, Y. Zhang and Z. Zhang for technical assistance, Drs. R. Patient of University of Oxford and N. Itoh of Kyoto University Graduate School of Pharmaceutical Sciences for *in situ* probes, Drs. R. Bernards of Division of Molecular Carcinogenesis and Center of Biomedical Genetics, The Netherlands Cancer Institute, and S. Gaubatz of Institute for Molecular Biology and Tumor Research, Philipps-University Marburg for *E2Fs* expression plasmids. This work was supported by 973 Project of National Key Basic Research (2007CB947100, 2006CB806605, 2006CB943802), grants from the Shanghai government (06dj14010, 07pj14107).

Appendix A. Supplementary data

Supplementary data associated with this article can be found, in the online version, at doi:10.1016/j.ydbio.2009.12.018.

References

Amatruda, J.F., Zon, L.I., 1999. Dissecting hematopoiesis and disease using the zebrafish. Dev. Biol. 216, 1–15.

Bennett, C.M., Kanki, J.P., Rhodes, J., Liu, T.X., Paw, B.H., Kieran, M.W., Langenau, D.M., Delahaye-Brown, A., Zon, L.I., Fleming, M.D., Look, A.T., 2001. Myelopoiesis in the zebrafish, *Danio rerio*. Blood 98, 643–651.

Berghmans, S., Murphey, R.D., Wienholds, E., Neuberg, D., Kutok, J.L., Fletcher, C.D., Morris, J.P., Liu, T.X., Schulte-Merker, S., Kanki, J.P., Plasterk, R., Zon, L.I., Look, A.T., 2005. tp53 mutant zebrafish develop malignant peripheral nerve sheath tumors. Proc. Natl. Acad. Sci. U. S. A. 102, 407–412.

Bill, B.R., Balciunas, D., McCarra, J.A., Young, E.D., Xiong, T., Spahn, A.M., Garcia-Lecea, M., Korzh, V., Ekker, S.C., Schimmenti, L.A., 2008. Development and Notch signaling requirements of the zebrafish choroid plexus. PLoS ONE e3114, 3.

Boerkoel, C.F., O'Neill, S., Andre, J.L., Benke, P.J., Bogdanovic, R., Bulla, M., Burguet, A., Cockfield, S., Cordeiro, I., Ehrich, J.H., Frund, S., Geary, D.F., Ieshima, A., Illies, F., Joseph, M.W., Kaitila, I., Lama, G., Leheup, B., Ludman, M.D., McLeod, D.R., Medeira, A., Milford, D.V., Ormala, T., Rener-Primec, Z., Santava, A., Santos, H.G., Schmidt, B., Smith, G.C., Spranger, J., Zupancic, N., Weksberg, R., 2000. Manifestations and treatment of Schimke immuno-osseous dysplasia: 14 new cases and a review of the literature. Eur. J. Pediatr. 159, 1–7.

Boerkoel, C.F., Takashima, H., John, J., Yan, J., Stankiewicz, P., Rosenbarker, L., Andre, J.L., Bogdanovic, R., Burguet, A., Cockfield, S., Cordeiro, I., Frund, S., Illies, F., Joseph, M., Kaitila, I., Lama, G., Loirat, C., McLeod, D.R., Milford, D.V., Petty, E.M., Rodrigo, F., Saraiva, J.M., Schmidt, B., Smith, G.C., Spranger, J., Stein, A., Thiele, H., Tizard, J., Weksberg, R., Lupski, J.R., Stockton, D.W., 2002. Mutant chromatin remodeling protein SMARCAL1 causes Schimke immuno-osseous dysplasia. Nat. Genet. 30, 215–220.

Bokenkamp, A., deJong, M., van Wijk, J.A., Block, D., van Hagen, J.M., Ludwig, M., 2005. R561C missense mutation in the SMARCAL1 gene associated with mild Schimke immuno-osseous dysplasia. Pediatr. Nephrol. 20, 1724–1728.

Cheung, K.J., Badarinarayana, V., Selinger, D.W., Janse, D., Church, G.M., 2003. A microarray-based antibiotic screen identifies a regulatory role for supercoiling in the osmotic stress response of *Escherichia coli*. Genome. Res. 13, 206–215.

Cho, K.R., Hedrick, L., 1997. Genetic alterations in human tumors. Curr. Top. Microbiol. Immunol. 221, 149–176.

Cho, K.S., Elizondo, L.I., Boerkoel, C.F., 2004. Advances in chromatin remodeling and human disease. Curr. Opin. Genet. Dev. 14, 308–315.

Clewing, J.M., Antalfy, B.C., Lucke, T., Najafian, B., Marwedel, K.M., Hori, A., Powel, R.M., Do, A.F., Najera, L., SantaCruz, K., Hicks, M.J., Armstrong, D.L., Boerkoel, C.F., 2007a. Schimke immuno-osseous dysplasia: a clinicopathological correlation. J. Med. Genet. 44, 122–130.

Clewing, J.M., Fryssira, H., Goodman, D., Smithson, S.F., Sloan, E.A., Lou, S., Huang, Y., Choi, K., Lucke, T., Alpay, H., Andre, J.L., Asakura, Y., Biebuyck-Gouge, N., Bogdanovic, R., Bonneau, D., Cancrini, C., Cochat, P., Cockfield, S., Collard, L.,

Cordeiro, I., Cormier-Daire, V., Cransberg, K., Cutka, K., Deschenes, G., Ehrich, J.H., Frund, S., Georgaki, H., Guillen-Navarro, E., Hinkelmann, B., Kanariou, M., Kasap, B., Kilic, S.S., Lama, G., Lamfers, P., Loirat, C., Majore, S., Milford, D., Morin, D., Ozdemir, N., Pontz, B.F., Proesmans, W., Psoni, S., Reichenbach, H., Reif, S., Rusu, C., Saraiva, J.M., Sakallioglu, O., Schmidt, B., Shoemaker, L., Sigaudy, S., Smith, G., Sotsiou, F., Stajic, N., Stein, A., Stray-Pedersen, A., Taha, D., Taque, S., Tizard, J., Tsimaratos, M., Wong, N.A., Boerkoel, C.F., 2007b. Schimke immunoosseous dysplasia: suggestions of genetic diversity. Hum. Mutat. 28, 273–283.

Coleman, M.A., Eisen, J.A., Mohrenweiser, H.W., 2000. Cloning and characterization of HARP/SMARCAL1: a prokaryotic HepA-related SNF2 helicase protein from human and mouse. Genomics 65, 274–282.

Dai, X., Rothman-Denes, L.B., 1999. DNA structure and transcription. Curr. Opin. Microbiol. 2, 126–130.

DeGregori, J., Johnson, D.G., 2006. Distinct and overlapping roles for E2F family members in transcription, proliferation and apoptosis. Curr. Mol. Med. 6, 739–748.

Deguchi, K., Clewing, J.M., Elizondo, L.I., Hirano, R., Huang, C., Choi, K., Sloan, E.A., Lucke, T., Marwedel, K.M., Powell Jr., R.D., Santa Cruz, K., Willaime-Morawek, S., Inoue, K., Lou, S., Northrop, J.L., Kanemura, Y., van der Kooy, D., Okano, H., Armstrong, D.L., Boerkoel, C.F., 2008. Neurologic phenotype of Schimke immuno-osseous dysplasia and neurodevelopmental expression of SMARCAL1. J. Neuropathol. Exp. Neurol. 67, 565–577.

Dooley, K., Zon, L.I., 2000. Zebrafish: a model system for the study of human disease. Curr. Opin. Genet. Dev. 10, 252–256.

Eisen, J.S., Smith, J.C., 2008. Controlling morpholino experiments: don't stop making antisense. Development 135, 1735–1743.

Ekker, S.C., Larson, J.D., 2001. Morphant technology in model developmental systems. Genesis 30, 89–93.

Elizondo, L.I., Huang, C., Northrop, J.L., Deguchi, K., Clewing, J.M., Armstrong, D.L., Boerkoel, C.F., 2006. Schimke immuno-osseous dysplasia: a cell autonomous disorder? Am. J. Med. Genet. A 140, 340–348.

Felsenstein, J., 2008. Comparative methods with sampling error and within-species variation: contrasts revisited and revised. Am. Nat. 171, 713–725.

Gabellini, C., Del Bufalo, D., Zupi, G., 2006. Involvement of RB gene family in tumor angiogenesis. Oncogene 25, 5326–5332.

Gamse, J.T., Shen, Y.C., Thisse, C., Thisse, B., Raymond, P.A., Halpern, M.E., Liang, J.O., 2002. Otx5 regulates genes that show circadian expression in the zebrafish pineal complex. Nat. Genet. 30, 117–121.

Gangaraju, V.K., Bartholomew, B., 2007. Mechanisms of ATP dependent chromatin remodeling. Mutat. Res. 618, 3–17.

Gering, M., Patient, R., 2005. Hedgehog signaling is required for adult blood stem cell formation in zebrafish embryos. Dev. Cell 8, 389–400.

Gongal, P.A., Waskiewicz, A.J., 2008. Zebrafish model of holoprosencephaly demonstrates a key role for TGIF in regulating retinoic acid metabolism. Hum. Mol. Genet. 17, 525–538.

Griffin, C.T., Brennan, J., Magnuson, T., 2008. The chromatin-remodeling enzyme BRG1 plays an essential role in primitive erythropoiesis and vascular development. Development 135, 493–500.

Hendzel, M.J., Wei, Y., Mancini, M.A., Van Hooser, A., Ranalli, T., Brinkley, B.R., Bazett-Jones, D.P., Allis, C.D., 1997. Mitosis-specific phosphorylation of histone H3 initiates primarily within pericentromeric heterochromatin during G2 and spreads in an ordered fashion coincident with mitotic chromosome condensation. Chromosoma 106, 348–360.

Horsfield, J.A., Anagnostou, S.H., Hu, J.K., Cho, K.H., Geisler, R., Lieschke, G., Crosier, K.E., Crosier, P.S., 2007. Cohesin-dependent regulation of Runx genes. Development 134, 2639–2649.

Huang, C., Sloan, E.A., Boerkoel, C.F., 2003. Chromatin remodeling and human disease. Curr. Opin. Genet. Dev. 13, 246–252.

Huang, C., Zhang, Y., Gong, Z., Sheng, X., Li, Z., Zhang, W., Qin, Y., 2006. Berberine inhibits 3T3-L1 adipocyte differentiation through the PPARgamma pathway. Biochem. Biophys. Res. Commun. 348, 571–578.

Isogai, S., Lawson, N.D., Torrealday, S., Horiguchi, M., Weinstein, B.M., 2003. Angiogenic network formation in the developing vertebrate trunk. Development 130, 5281–5290.

Iuchi, I., Yamamoto, M., 1983. Erythropoiesis in the developing rainbow trout, *Salmo gairdneri irideus*: histochemical and immunochemical detection of erythropoietic organs. J. Exp. Zool. 226, 409–417.

Jia, S., Ren, Z., Li, X., Zheng, Y., Meng, A., 2008. smad2 and smad3 are required for mesendoderm induction by transforming growth factor-beta/nodal signals in zebrafish. J. Biol. Chem. 283, 2418–2426.

Kadam, S., Emerson, B.M., 2002. Mechanisms of chromatin assembly and transcription. Curr. Opin. Cell Biol. 14, 262–268.

Kalev-Zylinska, M.L., Horsfield, J.A., Flores, M.V., Postlethwait, J.H., Vitas, M.R., Baas, A. M., Crosier, P.S., Crosier, K.E., 2002. Runx1 is required for zebrafish blood and vessel development and expression of a human RUNX1-CBF2T1 transgene advances a model for studies of leukemogenesis. Development 129, 2015–2030.

Korenjak, M., Brehm, A., 2005. E2F-Rb complexes regulating transcription of genes important for differentiation and development. Curr. Opin. Genet. Dev. 15, 520–527.

Koshida, S., Shinya, M., Mizuno, T., Kuroiwa, A., Takeda, H., 1998. Initial anteroposterior pattern of the zebrafish central nervous system is determined by differential competence of the epiblast. Development 125, 1957–1966.

Kumar, S., Tamura, K., Nei, M., 2004. MEGA3: integrated software for molecular evolutionary genetics analysis and sequence alignment. Brief. Bioinform. 5, 150–163.

Lam, E.Y., Chau, J.Y., Kalev-Zylinska, M.L., Fountaine, T.M., Mead, R.S., Hall, C.J., Crosier, P.S., Crosier, K.E., Flores, M.V., 2009. Zebrafish runx1 promoter-EGFP transgenics mark discrete sites of definitive blood progenitors. Blood 113, 1241–1249.

Langenau, D.M., Zon, L.I., 2005. The zebrafish: a new model of T-cell and thymic development. Nat. Rev. Immunol. 5, 307–317.

Lehner, C.F., O'Farrell, P.H., 1989. Expression and function of Drosophila cyclin A during embryonic cell cycle progression. Cell 56, 957–968.

Lim, H.M., Lewis, D.E., Lee, H.J., Liu, M., Adhya, S., 2003. Effect of varying the supercoiling of DNA on transcription and its regulation. Biochemistry 42, 10718–10725.

Liu, T.X., Howlett, N.G., Deng, M., Langenau, D.M., Hsu, K., Rhodes, J., Kanki, J.P., D'Andrea, A.D., Look, A.T., 2003. Knockdown of zebrafish Fancd2 causes developmental abnormalities via p53-dependent apoptosis. Dev. Cell 5, 903–914.

MacLachlan, T.K., El-Deiry, W.S., 2002. Apoptotic threshold is lowered by p53 transactivation of caspase-6. Proc. Natl. Acad. Sci. U. S. A. 99, 9492–9497.

Maroon, H., Walshe, J., Mahmood, R., Kiefer, P., Dickson, C., Mason, I., 2002. Fgf3 and Fgf8 are required together for formation of the otic placode and vesicle. Development 129, 2099–2108.

McReynolds, L.J., Gupta, S., Figueroa, M.E., Mullins, M.C., Evans, T., 2007. Smad1 and Smad5 differentially regulate embryonic hematopoiesis. Blood 110, 3881–3890.

Nasevicius, A., Ekker, S.C., 2000. Effective targeted gene 'knockdown' in zebrafish. Nat. Genet. 26, 216–220.

Nicoli, S., Presta, M., 2007. The zebrafish/tumor xenograft angiogenesis assay. Nat. Protoc. 2, 2918–2923.

Ogawa, H., Ishiguro, K., Gaubatz, S., Livingston, D.M., Nakatani, Y., 2002. A complex with chromatin modifiers that occupies E2F-and Myc-responsive genes in G0 cells. Science 296, 1132–1136.

Patterson, L.J., Gering, M., Eckfeldt, C.E., Green, A.R., Verfaillie, C.M., Ekker, S.C., Patient, R., 2007. The transcription factors Scl and Lmo2 act together during development of the hemangioblast in zebrafish. Blood 109, 2389–2398.

Ransom, D.G., Haffter, P., Odenthal, J., Brownlie, A., Vogelsang, E., Kelsh, R.N., Brand, M., van Eeden, F.J., Furutani-Seiki, M., Granato, M., Hammerschmidt, M., Heisenberg, C.P., Jiang, Y.J., Kane, D.A., Mullins, M.C., Nusslein-Volhard, C., 1996. Characterization of zebrafish mutants with defects in embryonic hematopoiesis. Development 123, 311–319.

Robu, M.E., Larson, J.D., Nasevicius, A., Beiraghi, S., Brenner, C., Farber, S.A., Ekker, S.C., 2007. p53 activation by knockdown technologies. PLoS Genet. 3, e78.

Salmon, K., Hung, S.P., Mekjian, K., Baldi, P., Hatfield, G.W., Gunsalus, R.P., 2003. Global gene expression profiling in *Escherichia coli* K12. The effects of oxygen availability and FNR. J. Biol. Chem. 278, 29837–29855.

Sawalha, A.H., 2008. Epigenetics and T-cell immunity. Autoimmunity 41, 245–252.

Shepard, J.L., Stern, H.M., Pfaff, K.L., Amatruda, J.F., 2004. Analysis of the cell cycle in zebrafish embryos. Methods Cell Biol. 76, 109–125.

Sprenger, F., Yakubovich, N., O'Farrell, P.H., 1997. S-phase function of Drosophila cyclin A and its downregulation in G1 phase. Curr. Biol. 7, 488–499.

Trimarchi, J.M., Fairchild, B., Verona, R., Moberg, K., Andon, N., Lees, J.A., 1998. E2F-6, a member of the E2F family that can behave as a transcriptional repressor. Proc. Natl. Acad. Sci. U. S. A. 95, 2850–2855.

Vidal, A., Koff, A., 2000. Cell-cycle inhibitors: three families united by a common cause. Gene 247, 1–15.

Wang, G.G., Allis, C.D., Chi, P., 2007. Chromatin remodeling and cancer, Part II: ATP-dependent chromatin remodeling. Trends Mol. Med. 13, 373–380.

Wu, L., Timmers, C., Maiti, B., Saavedra, H.I., Sang, L., Chong, G.T., Nuckolls, F., Giangrande, P., Wright, F.A., Field, S.J., Greenberg, M.E., Orkin, S., Nevins, J.R., Robinson, M.L., Leone, G., 2001. The E2F1-3 transcription factors are essential for cellular proliferation. Nature 414, 457–462.

Yamauchi, H., Hotta, Y., Konishi, M., Miyake, A., Kawahara, A., Itoh, N., 2006. Fgf21 is essential for haematopoiesis in zebrafish. EMBO Rep. 7, 649–654.

Yoshida, T., Hazan, I., Zhang, J., Ng, S.Y., Naito, T., Snippert, H.J., Heller, E.J., Qi, X., Lawton, L.N., Williams, C.J., Georgopoulos, K., 2008. The role of the chromatin remodeler Mi-2beta in hematopoietic stem cell self-renewal and multilineage differentiation. Genes Dev. 22, 1174–1189.

Yusufzai, T., Kadonaga, J.T., 2008. HARP is an ATP-driven annealing helicase. Science 322, 748–750.